FEMS Microbiology Ecology, 91, 2015, fiv027

doi: 10.1093/femsec/fiv027
Advance Access Publication Date: 16 March 2015
Research Article

RESEARCH ARTICLE

The carbon starvation response of the ectomycorrhizal fungus *Paxillus involutus*

Magnus Ellström[1,2], Firoz Shah[1], Tomas Johansson[1], Dag Ahrén[1,3], Per Persson[1,2] and Anders Tunlid[1,*]

[1]Microbial Ecology, Department of Biology, Lund University, Ecology Building, SE 223 62 Lund, Sweden, [2]Centre for Environmental and Climate Research (CEC), Lund University, Ecology Building, SE 223 62 Lund, Sweden and [3]BILS Bioinformatics Infrastructure for Life Sciences, Department of Biology, Lund University, Ecology Building, SE 223 62 Lund, Sweden

*Corresponding author: Department of Biology, Lund University, Ecology Building, SE 223 62 Lund, Sweden. Tel: +46-462223757; E-mail: anders.tunlid@biol.lu.se

One sentence summary: The mycelium of an ectomycorrhizal fungus responds rapidly to carbon starvation by disruptions of cell walls and release of cellular material.

Editor: Ian C Anderson

ABSTRACT

The amounts of carbon allocated to the fungal partner in ectomycorrhizal associations can vary substantially depending on the plant growth and the soil nutrient conditions, and the fungus may frequently be confronted with limitations in carbon. We used chemical analysis and transcriptome profiling to examine the physiological response of the ectomycorrhizal fungus *Paxillus involutus* to carbon starvation during axenic cultivation. Carbon starvation induced a decrease in the biomass. Concomitantly, ammonium, cell wall material (chitin) and proteolytic enzymes were released into the medium, which suggest autolysis. Compared with the transcriptome of actively growing hyphae, about 45% of the transcripts analyzed were differentially regulated during C-starvation. Induced during starvation were transcripts encoding extracellular enzymes such as peptidases, chitinases and laccases. In parallel, transcripts of N-transporters were upregulated, which suggest that some of the released nitrogen compounds were re-assimilated by the mycelium. The observed changes suggest that the carbon starvation response in *P. involutus* is associated with complex cellular changes that involves autolysis, recycling of intracellular compounds by autophagy and reabsorption of the extracellular released material. The study provides molecular markers that can be used to examine the role of autolysis for the turnover and survival of the ectomycorrhizal mycelium in soils.

Keywords: autolysis; autophagy; ammonium release; basidiomycete; transcriptome

INTRODUCTION

Most boreal and northern temperate forest tree species live in symbiosis with ectomycorrhizal (ECM) fungi (Smith and Read 2008). In these ecologically important associations, the fungus provides the plant with mineral nutrients, and in return the plant supplies the fungus with photosynthetically derived carbohydrates. This carbon (C) supports the growth of an extramatrical mycelium (EMM) (Smith and Read 2008). It is known that the growth and turnover of the EMM is dependent on the plant C (Högberg and Högberg 2002; Högberg *et al.* 2010). A laboratory study by Leake *et al.* (2001) showed, using ^{14}C pulse labeling of tree seedlings, that the plant C was rapidly allocated through the EMM network and preferentially to the mycelium colonizing

Received: 2 January 2015; **Accepted:** 10 March 2015

litter patches in the soil. When the mycelium had assimilated the nutrients, the flow of plant C ceased and the biomass of the mycelium in the litter patches declined. The plant C supply for EMM production can be affected by many biotic and abiotic factors, such as plant properties, forest management, growth season, nutrient conditions in the soil and global change including elevated CO_2 levels and increased nitrogen (N) deposition (Ericsson 1995; Högberg *et al.* 2010; Ekblad *et al.* 2013). For example, both field studies (Arnebrant and Söderström 1992; Kjøller *et al.* 2012; Bahr *et al.* 2013) and microcosm studies (Wallander and Nylund 1992; Arnebrant 1994) have shown that the biomass of EMM decreases under increased N loads.

The physiological mechanisms by which ECM fungi respond to conditions of reduced C supplies are poorly characterized. However, there have been studies of this process in other kinds of filamentous fungi, particularly in industrially important fungi, such as the ascomycetes *Aspergillus niger* and *Penicillium chrysogenum*, and in the model species *Aspergillus nidulans* (White *et al.* 2002; Shin *et al.* 2009; Nitsche *et al.* 2012). C-starvation in these fungi leads to autolysis, autophagy and recycling of nutrients (White *et al.* 2002; Pocsi *et al.* 2003; Sami *et al.* 2003; Nitsche *et al.* 2012; Nitsche *et al.* 2013).

Autolysis is the multistage self-degradation of cells by hydrolytic enzymes, which leads to leakage of intracellular material (White *et al.* 2002; Shin *et al.* 2009). It involves a reduction in biomass, release of ammonium and production of cell wall hydrolytic enzymes and proteases (Nitsche *et al.* 2012). Autolysis is induced not only by C-starvation but also by limitations in other nutrients, physical stress and aging (White *et al.* 2002; Shin *et al.* 2009). It can promote the survival of the mycelium, because actively growing hyphal tips can assimilate the organic compounds liberated from the lysing parts of the culture (Schrickx *et al.* 1993; White *et al.* 2002), a process called cryptic growth (Trinci and Righelato 1970; White *et al.* 2002).

Autophagy is a conserved recycling process found in all eukaryotic cells in which intracellular components are degraded within the vacuole and the resulting compounds are recycled (Pollack, Harris and Marten 2009; Sharon *et al.* 2009; Feng *et al.* 2014). The term autophagy can refer to several different phenomena; it can be divided into macro- and microautophagy and can be either selective or non-selective (Pollack, Harris and Marten 2009). Microautophagy is the direct introversion of cytosolic material into the vacuole whereas macroautophagy is the engulfment of cytosolic material by autophagosomes, which subsequently fuse with the vacuole (Pollack, Harris and Marten 2009). Hereafter in this paper, we use autophagy to mean macroautophagy. The autophagy pathways are highly conserved in eukaryotes, and to date over 30 autophagy-related (*atg*) genes have been identified in *Saccharomyces cerevisiae* (Voigt and Poeggeler 2013; Feng *et al.* 2014). In filamentous fungi, autophagy appears to be involved in nutrient recycling during nutrient starvation and in cellular differentiation (Pollack, Harris and Marten 2009). C-starvation in *A. niger* and *A. nidulans* is accompanied by the induction of genes related to autophagy (Nitsche *et al.* 2012; Szilagyi *et al.* 2013). Most likely, autophagy has an important role in nutrient recycling during C-starvation in these fungi. In addition, studies using *A. niger atg* mutants suggest that autophagy promotes the survival of the mycelium during C depletion by organelle turnover and protection against cell death (Nitsche *et al.* 2013).

In this study, we have investigated the physiological response to C-starvation by the EMF *Paxillus involutus*, by using biochemical analyses and transcriptome profiling. *Paxillus involutus* is a common ECM basidiomycete, widely distributed throughout the Northern Hemisphere and forms ectomycorrhizae with numerous coniferous and deciduous tree species (Wallander and Söderström 1999). In particular, we assessed whether the physiological and transcriptional changes caused by carbon starvation in *P. involutus* in axenic cultures is similar to those observed in well-studied ascomycetes; and whether at least some of the released cellular components can be recycled by autophagy, degradation and assimilation. The study is the first system-wide analysis of the carbon starvation response in an ECM fungus and provides molecular markers that can be used to examine the role of autolysis for the turnover and survival of the ECM mycelium in soils.

MATERIALS AND METHODS

Fungal strain and culture conditions

Cultures of *P. involutus* (Batsch) Fr. (strain ATCC 200175 (www.atcc.org)) (Basidiomycota, Boletales) were maintained aseptically on 1.5% agar plates containing Modified Melin–Norkrans (MMN) medium (composition: 2.5 g l^{-1} glucose, 500 mg l^{-1} KH_2PO_4, 250 mg l^{-1} $(NH_4)_2HPO_4$, 150 mg l^{-1} $MgSO_4 \times 7H_2O$, 25 mg l^{-1} NaCl, 50 mg l^{-1} $CaCl_2 \times 2H_2O$, 12 mg l^{-1} $FeCl_3 \times 6H_2O$ and 1 mg l^{-1} thiamine-HCl; pH 4.0, C/N ratio 18). Inoculum pieces (5 × 5 mm) of *P. involutus*, from the edge of 7-day-old actively growing cultures, were transferred to Petri dishes (diameter 10 cm) containing 10 ml of liquid MMN medium and a monolayer of glass beads (diameter 4 mm) for fungal growth support (Rineau *et al.* 2012). All cultures were kept in the dark at 18°C throughout the experiment. After 10 days of incubation, the liquid MMN medium was replaced with liquid MMN medium without $(NH_4)_2HPO_4$ (pH 3.3) to produce an N-deprived mycelia (Shah *et al.* 2013). After 24 h, the MMN medium was replaced with new liquid MMN medium modified to 1.5 g l^{-1} $(NH_4)_2HPO_4$, generating a C/N ratio of 3. The cultures were incubated for 15 days. At seven time points (day 0, 2, 6, 8, 10, 13 and 15), fungal mycelia and liquid media from three Petri dishes (three biological replicates) were collected for analysis.

At the time of harvest, the diameter of each culture was measured. Each mycelium was collected, rinsed in MilliQ water and lyophilized. The dry weight of the mycelium was subsequently measured. The liquid culture medium was stored at –20°C until analysis.

Chemical analyses

Glucose content of the culture medium was measured colorimetrically using the Glucose Assay Kit (GO) (Sigma-Aldrich, Germany). Ammonium in the culture medium was measured by flow injection analysis (FIA) using an FIAstar 5000 Analyzer (Foss Tecator, Sweden).

The culture medium was analyzed using ATR-FTIR (attenuated total reflectance-Fourier transform infrared) spectroscopy. A total of 20 μl of the culture medium, which had been vacuum concentrated from 1 ml to 50 μl using an AES 1000 SpeedVac (Thermo Scientific, USA), was allowed to evaporate on an ATR crystal (ZnSe, Harrick Scientific Products Inc. USA). The FTIR spectrum was recorded using a Vertex 80v (Bruker, USA) set at continuous sampling and each spectrum was the result of 300 consecutive scans at a resolution of 4 cm^{-1}. The spectrum of the sample in close contact with the ATR crystal was recorded continuously every 5 min until no change in the spectrum was detectable; this change was primarily related to water evaporation.

The chemical changes in the culture medium were also assayed using synchronous fluorescence spectroscopy. The spectra were obtained using an LS50B fluorescence spectrometer (Perkin Elmer, USA) set at 10 nm bandwidth and 25 nm offset (Dl = 25 nm) between excitation and emission.

The concentration of chitin in the medium was measured colorimetrically as previously described (Tsuji, Kinoshita and Hoshino 1969; Plassard, Mousain and Salsac 1982) with the following modification to volumes. One milliliter of lyophilized liquid growth media was hydrolyzed overnight in 100 μl 6 N HCl at 80°C, transforming chitin to glucosamine. After the hydrolysis, 500 μl 1.25 M Na acetate was added to the sample to increase the pH to 3.0. A method previously described (Tsuji, Kinoshita and Hoshino 1969) was then followed using 5-fold reduced volumes, keeping all ratios unaltered. Known concentrations (1–100 μg ml^{-1}) of chitosan (Fluka, Switzerland), dissolved in 1% acetic acid (v/v) were lyophilized and used as standard.

Proteolytic activity was measured using a modified fluorescent method as previously described (Twining 1984; Shah *et al.* 2013). Fluorescence was measured using an LS50B fluorescence spectrometer (Perkin Elmer) with excitation set to 490 nm and emission set to 525 nm. The protease activity is expressed in trypsin equivalents: one trypsin equivalent corresponds to the fluorescence produced by 1 μg ml^{-1} of trypsin (Sigma-Aldrich, Germany).

RNA extraction and microarray analysis

Fungal mycelia from four of the time points representing different growth stages: active growth phase (AG, day 2), onset of C-starvation (CS (O), day 6), medium C-starvation (CS (M), day 8) and late C-starvation (CS (L), day 13) were collected. From each time point three biological replicates were collected (for each replicate, mycelia from two Petri dishes were pooled). The mycelia were immediately submerged in liquid N, ground to a fine powder, and stored at –80°C. Total RNA was isolated using the RNeasy Plant Mini Kit (Qiagen, USA) using the RLC buffer and the on-column DNase treatment according to the manufacturer's instructions. Total RNA was eluted in H_2O and stored at –20°C. For quality assessments, all samples were inspected using an RNA 6000 Nano kit on a 2100 Bioanalyzer (Agilent, USA).

Transcriptional profiling was performed using a custom-designed microarray (12-plex 135K-oligonucleotide microarray, DesignID: 546871; NimbleGen/Roche, Switzerland) containing probes representing 12 214 transcripts (isotigs) that had been obtained by 454/Roche DNA sequencing and Sanger sequencing (Applied BioSystems, USA) of a number of *P. involutus* transcriptomes collected during growth on various organic matter extracts and MMN medium (Rineau *et al.* 2012). Each isotig is represented by up to 10 probes (60-mers) in a tiled design, which is deposited at NCBI Gene Expression Omnibus (GEO accession GPL14950; Edgar, Domrachev and Lash 2002; Ball *et al.* 2004). Isotig sequence information and putative annotations are available from the Paxillus EST database: http://mbio-serv2.mbioekol.lu.se/Paxillus/Hybrid/ (add 'paxillus_' to the isotig ID when searching).

The microarray analyses were performed as single-label hybridizations. For each hybridization and each sample, 10 μg total RNA was used for cDNA synthesis using the SuperScript Double-Stranded cDNA Synthesis Kit (Invitrogen, USA) according to the manufacturer's instructions. Quality of the produced cDNA was assessed using a High Sensitivity DNA Kit on a 2100 Bioanalyzer (Agilent). Samples were labeled using a One-Color DNA Labeling Kit (Cy3) (NimbleGen/Roche) according to the manufacturer's instructions. After labeling, each sample received a Sample Tracking Control (NimbleGen/Roche) and hybridizations were immediately performed in a Hybridization System 4 (NimbleGen/Roche) for at least 16 h according to the manufacturer's instructions. The washing procedure was performed according to the manufacturer's instructions (NimbleGen/Roche) and the slides were finally scanned using an Agilent High-Resolution Microarray Scanner set at 20% PMT and 2 μm of resolution. The raw images were bursted and processed using the NimbleScan software v8.0 (NimbleGen/Roche) and the built-in Robust Multichip Average (RMA) algorithm including quantile normalization for the purpose of removing the effects of systematic variation in the measured fluorescence intensities (Bolstad *et al.* 2003; Irizarry *et al.* 2003).

Principal component analysis (PCA) and statistical analyses were performed on normalized (log2-transformed) transcriptional values in Omics Explorer v2.2 (Qlucore, Sweden). The Bejmanini–Hochberger false discovery rate (q) was used to correct for multiple comparisons (Benjamini and Hochberg 1995). The transcriptional data have been deposited at NCBI GEO and are accessible through the GEO SuperSeries accession number GSE54940.

Bioinformatic analyses

Isotig sequences were annotated using information from the Paxillus EST database (see above). The database allows access to UniProt annotations (Apweiler *et al.* 2004) and Pfam domains (Finn *et al.* 2014). Isotigs encoding putative peptidases, N-transporters and enzymes and proteins with a possible role in the degradation of organic material were identified as previously described (Rineau *et al.* 2012; Rineau *et al.* 2013; Shah *et al.* 2013). Annotations of transcripts encoding enzymes active on carbohydrates (CAZymes) and those of auxiliary redox activities/enzymes (AAs) were retrieved from the Carbohydrate-Active Enzymes Database (http://www.cazy.org/) (Cantarel *et al.* 2009; Levasseur *et al.* 2013). Autophagy-related (*atg*) genes in the *P. involutus* genome were identified using annotation of such genes in the *Serpula lacrymans* and *A. niger* genomes (Eastwood *et al.* 2011; Nitsche *et al.* 2012). Relevant gene models were used as queries to identify putative homologs using the blastp tools available at the JGI *P. involutus* genome database (http://genome.jgi.doe.gov/Paxin1/Paxin1.home.html). Functional subgroups of the ATG proteins were inferred using information from Feng *et al.* (2014). Isotigs that were differentially expressed during C-starvation were mapped to the corresponding gene model in the *P. involutus* genome (Kohler *et al.* 2015) using blastn. In the manuscript, the protein models are designated Pi:XXXX. Predictions of putative secretory signals were conducted on protein models using SignalP 4.0 (Petersen *et al.* 2011).

Upregulated transcripts were revealed by comparison of expression levels from the different phases of starvation (CS (O), CS (M), CS (L)) with the levels in the actively growing (AG) mycelium (false discovery rate $q \leq 0.01$). Pfam enrichment analysis was done by calculating the number of occurrences of each Pfam domain in the proteins encoded by the upregulated transcripts and in the whole predicted proteome. Frequencies are given as the number of occurrences over the total number of Pfam domains among the upregulated and whole proteome. The probability (P) of observing the frequency of Pfam domains in the secretome and among the upregulated genes by chance was estimated using the hypergeometric distribution. Probabilities were corrected

for multiple testing using the Benjamini–Hochberg false discovery rate approach with a threshold of 0.10.

RESULTS

Induction of C-starvation

Transferring mycelium of *P. involutus* to medium with low C/N ratio induced an initial phase of active growth (Fig. 1a). The biomass and the radial growth of the mycelium increased during the first 6 days of incubation. At day 6, the biomass started to decline while the area of the mycelium continued to increase until ~10 days of growth. The uncoupled response in biomass and area suggests a thinning of the mycelium.

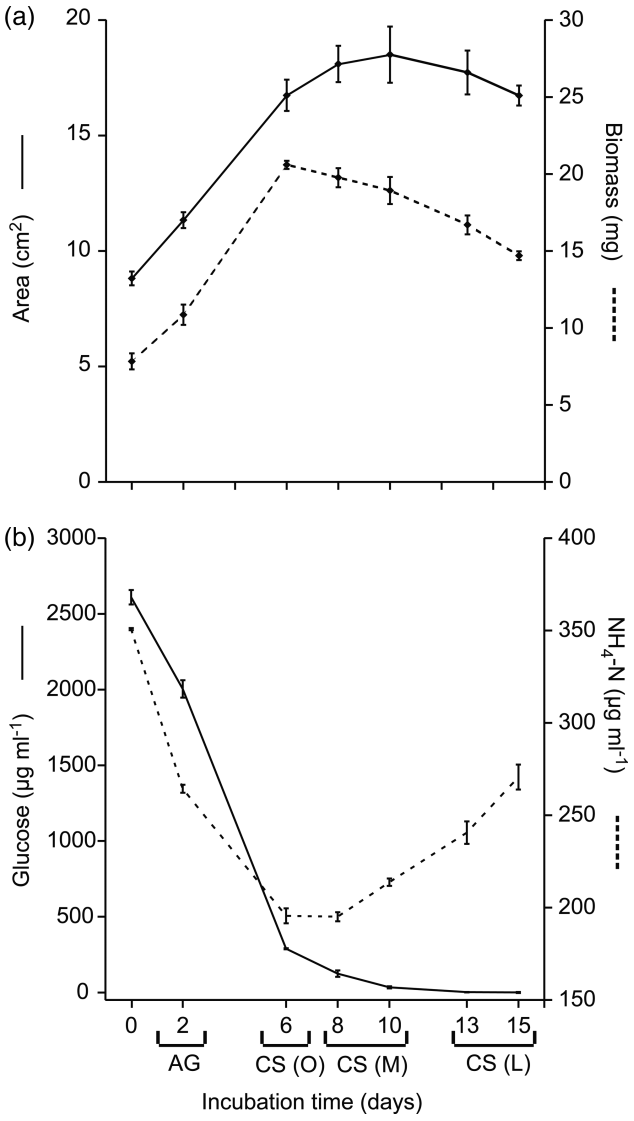

Figure 1. Induction of C-starvation in *P. involutus*. The fungus was grown on MMN medium (C/N ratio = 18) for 10 days. The medium was then replaced with a modified MMN medium having a C/N ratio of 3 and the mycelium was incubated for up to 15 days; times shown are days after the start of incubation. (**a**) Biomass and radial growth ($n = 3$, bars indicate SE). (**b**) Concentrations of glucose and ammonium in the medium ($n = 3$, bars indicate SE). (AG) denotes the active growth phase; CS (O), the onset of the C-starvation; CS (M), the medium C-starvation phase; CS (L), the late C-starvation phase.

During the initial phase of active growth, glucose and ammonium were assimilated from the medium by the fungus (Fig. 1b). At day 6, when the biomass started to decline, almost all glucose and a large part of the ammonium had been assimilated by the fungus (Fig. 1b). Thus, at day 6, the C source was no longer sufficient to maintain vegetative growth of the fungus, and we denoted samples from this day as being from the onset of the C-starvation phase (CS (O)). In the following days, concomitant with the decrease in biomass, ammonium was released into the medium and samples collected at day 8 and 10 were denoted as being from the medium C-starvation phase (CS (M)). Samples from day 13 and 15, when both the biomass and area of the mycelium were declining, were designated as being from the late C-starvation phase (CS (L)).

Release of compounds and peptidases in the medium

Analysis of the medium during C-starvation using synchronous fluorescence spectroscopy showed that there was a significant increase in the intensity of a peak located around 280–300 nm (Fig. 2a), which suggests that the fungus were releasing compounds containing monoaromatic functional groups like the amino-acids tyrosine, tryptophan and phenylalanine (Yamashita and Tanoue 2003).

Infrared spectra also indicated compositional changes of the growth medium during the C-starvation phase (Fig. 2b). The initial changes were primarily associated with the disappearance of glucose (bands at 1075, 1104 and 1150 cm^{-1}) in agreement with Fig. 1b. At the end of the starvation phase new bands appeared in the region 1400–1800 cm^{-1}, especially for day 15. The band around 1400 cm^{-1} could be related to the release of ammonium ions (Fig. 2b) whereas those between 1500–1800 cm^{-1} likely originated from biopolymers such as polysaccharides and proteins (Colthup, Daly and Wiberley 1990) (Fig. 2b, insert). The shoulders at 1555 and 1655 cm^{-1} were consistent with chitin (Brugnerotto *et al.* 2001), but the overlap with protein bands were substantial (Barth 2007). Thus, to verify the presence of chitin, the concentration of chitin in the culture filtrate was estimated using a colorimetric assay. The mean concentration of chitin at day 15 was 17.2 $\mu g\ ml^{-1}$ (SE = 2.5, $n = 2$) which is considerably higher than the concentration at earlier stages of the starvation [day 13: 6.2 $\mu g\ ml^{-1}$ (SE = 1.1, $n = 3$); day 10: 6.4 $\mu g\ ml^{-1}$ (SE = 1.4, $n = 3$); day 8: 7.0 $\mu g\ ml^{-1}$ (SE = 1.8, $n = 3$); day 6: 9.1 $\mu g\ ml^{-1}$ (SE = 2.5, $n = 3$)].

The proteolytic activity in the growth medium increased during C-starvation (Fig. 3). The highest level of extracellular proteolytic activity was detected at the late C-starvation phase.

Transcriptional response

RNA samples from the actively growing mycelium and the different phases of C-starvation were subjected to transcriptome analysis using a DNA microarray. A bioinformatics analysis showed that the microarray contained probes for 41% (7322 out of 17 968) of the predicted protein models in the genome sequence of *P. involutus* (Kohler *et al.* 2015) (Table S1, Supporting Information). The cohort of the 7322 proteins contained a large proportions of the genome models assigned to Eukaryotic Orthologous Groups (KOGs) (61% of all models with KOG assignments), enzymes with EC numbers (74%), proteins with Pfam domains (61%), CAZymes (63%), AAs (79%), peptidases (73%) and N-transporters (82%).

A PCA based on gene expression levels showed that C-starvation induced a distinct change in the transcriptome (Fig. 4a). The first axis (explaining 54% of the variability)

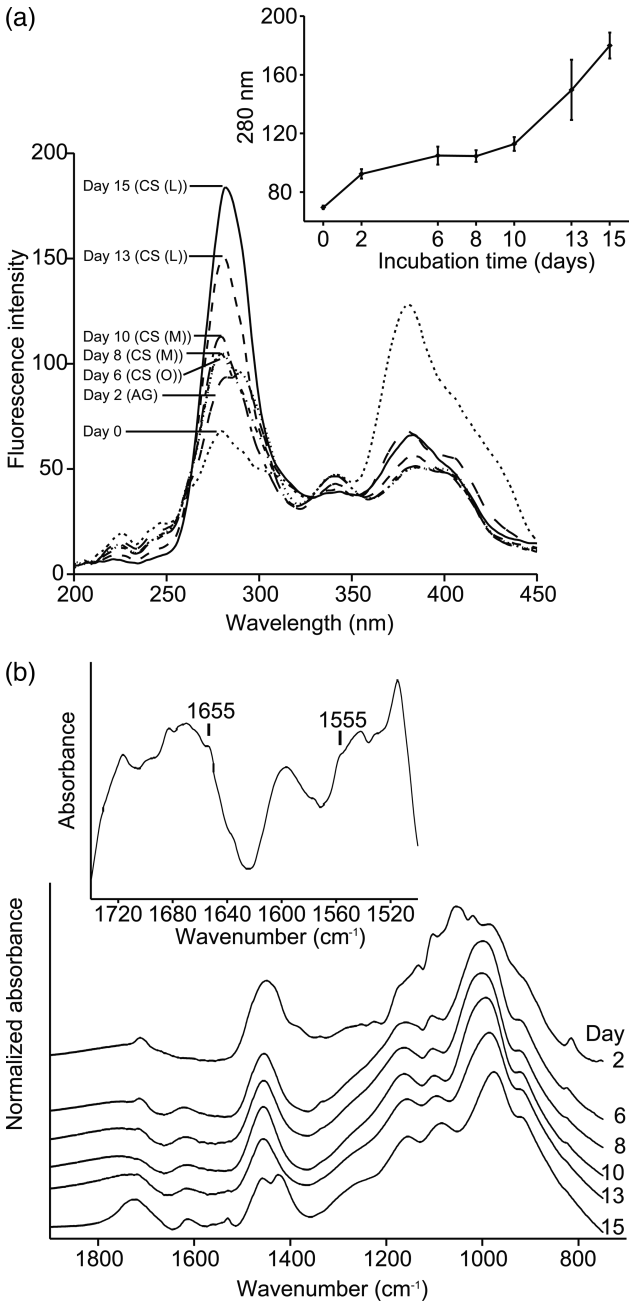

Figure 2. Analysis of compounds released into the medium during C-starvation. (a) Synchronous fluorescence spectroscopy. Inset shows the intensity change of the peak at 280 nm ($n = 3$, bars indicate SE). (b) FTIR-ATR spectroscopy. Inset shows the difference spectrum: spectrum (day 15)–spectrum (day 13). (AG) denotes the active growth phase; CS (O), the onset of the C-starvation; CS (M), the medium C-starvation phase; CS (L), the late C-starvation phase.

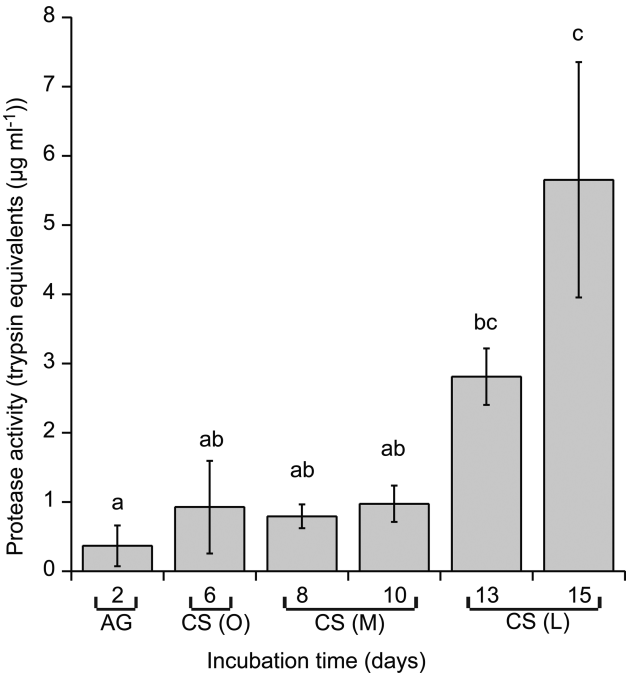

Figure 3. Proteolytic activity released into the media during C-starvation. Different letters indicate significant differences at the 0.05 level according to Tukey's post hoc test on log (sample + 1) transformed values ($n = 3$, bars indicate SE). (AG) denotes the active growth phase; CS (O), the onset of the C-starvation; CS (M), the medium C-starvation phase; CS (L), the late C-starvation phase.

separated the samples according to their time of C-starvation. The second axis (31%) separates the initial phases of C-starvation (CS (O) and CS (M)) from the AG and late stage of C-starvation (CS (L)). Compared with the active growth phase, 5498 of totally 12 214 transcripts (45%) were differentially expressed during at least one of the starvation phases (Fig. 4b). In total 1986 of the differentially expressed transcripts were up- or downregulated more than 2-fold; 194 transcripts were regulated more than 5-fold. Though, a majority of the regulated transcripts were differentially expressed at specific stages of the starvation, a fraction (723 out of 5498 transcripts) were commonly regulated during all stages (Fig. 4b). A large portion of the commonly regulated transcripts were found to encode proteins with basic cellular functions; 72% of these transcripts were assigned to KOGs, in contrast to 55% of the transcripts that were differentially regulated during starvation (Fig. S1, Supporting Information). The frequencies of transcripts assigned to the KOG classes 'Translation, ribosomal structure and biogenesis' and 'Replication, recombination and repair' were higher in the cohort of the commonly regulated genes than in the differentially regulated genes.

To get an insight into the biological functions that were enriched in *P. involutus* during C-starvation, we compared the frequency of occurrence of Pfam domains encoded by the upregulated transcripts with those of the proteome. We identified 21 Pfam domains to be enriched during C-starvation (Fig. 5). Among the enriched Pfam domains were those of transporters (amino-acid permease and the major facilitator superfamily), oxidases (multicopper oxidases and the cytochrome P450 superfamily of monoxidases), enzymes of fatty acid β-oxidation (acyl-CoA dehydrogenases) and transcription factors.

Secreted enzymes

Analyses of the most highly upregulated transcripts during C-starvation showed that many of them encoded extracellular enzymes such as hydrolases, oxidases and transferases (Fig. 6a). Among the hydrolases were four aspartate endopeptidases that were classified into two MEROPS A1 subfamilies: the polyporopepsin (A01.019) and the A01 assigned peptidases. A carboxypeptidase of the S10 subfamily was also upregulated. Three glycoside hydrolases of the GH10, GH18 and GH30 families were significantly upregulated. Family GH18 contains glycoside hydrolases that are both catalytically active chitinases

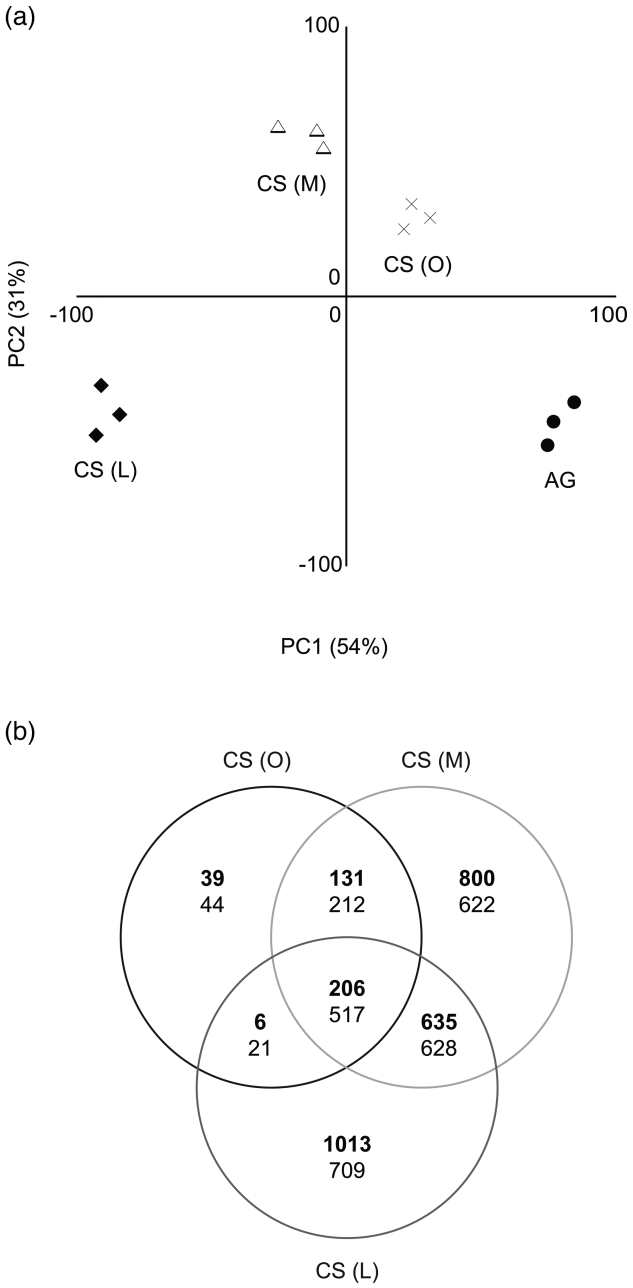

Figure 4. Transcriptional response during C-starvation in *P. involutus*. (**a**) PCA plot of the expression levels. The analysis was performed on the expression levels (log_2 normalized) of 7677 transcripts out of 12 214 that had a false discovery rate $q \leq 0.01$ ($n = 3$, *f*-test). Each point in the PCA represents a replicate from one of the different growth phases: active growth phase (AG, day 2), onset of C-starvation (CS (O), day 6), after 2 days (CS (M), day 8), and 7 days (CS (L), day 13) of starvation. (**b**) Venn diagram showing the number of upregulated transcripts (bold letters) and downregulated transcripts. Differential expression was revealed by pair-wise comparisons of expression levels from the different phases of starvation (CS (O), CS (M), CS (L)) with the levels in the actively growing mycelium (AG) ($q \leq 0.01$, $n = 3$, *t*-test). In total 5498 transcripts were differentially expressed during at least one of the starvation phases.

and endo-β-N-acetylglucosaminidases; family GH10 contains endoglucanases/exoglucanases and xylanases; and GH30 has members with three known enzyme activities: β-glucosylceramidase, β-1,6-glucanase and β-xylosidase (Cantarel *et al.* 2009). The most highly upregulated oxidases encompassed laccases, an oxidase containing the FAD domain and two members of the cytochrome P450 superfamily of monooxygenases.

N-transporters

We identified 14 N-transporters that were significantly upregulated at least 2-fold during C-starvation (Fig. 6b). Similar to the extracellular peptidases, the putative amino-acid transporters were most highly upregulated at the late stage of C-starvation. The upregulated N-transporters included several putative amino-acid and oligopeptide transporters (OPTs) including members of the amino-acid/polyamine/organocation (APC) transporter superfamily (which contains the amino-acid permease Pfam domain PF00324), the OPT superfamily and MFS transporters of the Drug:H^+ antiporter (DHA1 and DHA2) families (Fig. 6b). Similar to the extracellular peptidases, these transporters were most prominent at the late stages of C-starvation. A transcript encoding a putative ammonium transporter was also upregulated at this stage.

Autophagy-related proteins

Based on manual annotations, 20 putative *atg* genes were identified in the genome of *P. involutus*. Thirteen of these *atg* genes were significantly upregulated during C-starvation in *P. involutus* (Fig. 7). Ten of them encode proteins that are required for autophagosome formation, i.e. the core autophagy machinery (Feng *et al.* 2014). In addition, two of the upregulated *atg* genes are components of the cytoplasm-to-vacuole-targeting pathway.

DISCUSSION

Here, we have used chemical and transcriptomic profiling to investigate the response to C-starvation in the ECM basidiomycete *P. involutus*. The results suggest that this process in *P. involutus* is similar to that previously observed in saprophytic ascomycetes (White *et al.* 2002; Pocsi *et al.* 2003; Pollack, Harris and Marten 2009; Nitsche *et al.* 2012; Nitsche *et al.* 2013; Voigt and Poeggeler 2013): initiation of C-starvation-induced autolysis, autophagy and recycling of nutrients. Autolysis was revealed by the appearance of several morphological and molecular markers such as a reduction in biomass, degradation of hyphae, release of ammonium and production of hydrolytic enzymes such as chitinases and peptidases. During later stages of the starvation, components of the core autophagy machinery and various transporters for amino acids and peptides were upregulated which suggest that components released during autolysis can be recycled and hence promote the survival of the mycelium upon C-starvation.

During the early phase of C-starvation in ascomycetes it has been observed that the diameter of the growing hyphae decrease and the hyphal compartments become empty (White *et al.* 2002; Nitsche *et al.* 2012). Though, the morphological changes of the starving mycelium of *P. involutus* was not examined in detail, the observation that the biomass of the mycelium started to decline at the onset of C-starvation while the area continued to increase suggested that C-starvation induced a thinning of the mycelium. During the days following induction of C-starvation, chitin was released into the medium, probably due to fragmentation and/or hydrolysis of cell wall material. Among the upregulated transcripts encoding hydrolytic enzymes were two putative chitinases of the GH18 family, which might have a role in degrading the chitin present in the hyphae of the C-starving cultures of *P. involutus*. A strong transcriptional induction of chitinases during C-starvation has been observed in several

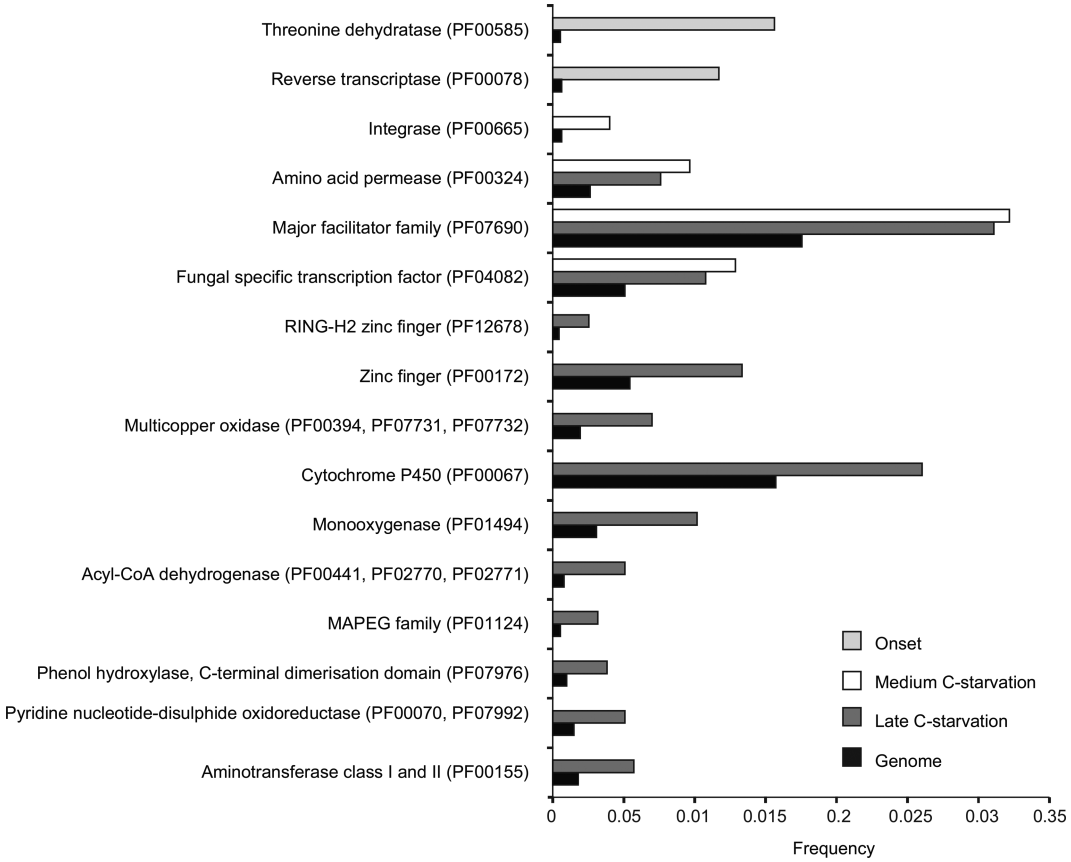

Figure 5. Pfam domains enriched during C-starvation in *P. involutus*. Shown are the frequencies of the Pfam domains that were significantly ($q < 0.10$, $n = 3$) enriched in the upregulated transcriptome in at least one of the pair-wise comparisons between mycelium at the onset of C-starvation, medium C-starvation phase, and the late C-starvation phase versus actively growing mycelium. 'Genome' refers to the frequencies of Pfam domain s in the whole proteome.

filamentous ascomycetes, such as *A. nidulans* and *A. niger* (Nitsche *et al.* 2012; Szilagyi *et al.* 2013).

The release of ammonium into the medium during C-starvation in *P. involutus* suggests that organic N-compounds were degraded and their C-skeletons were used for energy production. Both arginase (EC 3.5.3.1) and urease (3.5.1.5) were significantly upregulated at the time when ammonium was accumulated in the medium (Fig. S2, Supporting Information), suggesting that the ammonium was derived from the degradation of arginine and urea. An alternative pathway for the generation of ammonium is by the activity of glutamate dehydrogenase (EC 1.4.1.2), which catalyzes the deamination of glutamate to ammonium and oxoglutarate. However, this enzyme was not significantly upregulated during C-starvation in *P. involutus* (Fig. S2, Supporting Information). Hence, a large part of the released ammonium appears to originate from the hydrolysis of arginine and urea. The mechanism by which the produced ammonium is released into the medium by the C-starving mycelium of *P. involutus* is not known. Two candidates of transporters that could transfer ammonia from the cytosol to the medium are aquaporins and members of the Gpr1/Fun34/yaaH family; the latter includes the *ato2/ato3* (ammonium transporter outwards) genes of *S. cerevisiae* (Guaragnella and Butow 2003; Chalot, Blaudez and Brun 2006; Dietz *et al.* 2011). We identified two isotigs (13615 and 13585) displaying significant sequence similarity to *ato3/ato4* genes and three isotigs (5306, 3967 and 3969) encoding putative aquaporins. However, none of these transcripts were significantly regulated during C-starvation in *P. involutus* (data not shown). Hence, it is tempting to speculate that the ammonium is not secreted by transporters but is directly released into the medium from the lysed part of the mycelium.

Similarly to recent transcriptome analyses of *A. niger* (Nitsche *et al.* 2012) and *A. nidulans* (Szilagyi *et al.* 2013), the C-starvation response of *P. involutus* induced transcription of a number of genes encoding components of the autophagy machinery. Most of them are putative homologs of proteins known to be involved in non-selective autophagy and the formation of the autophagosome (Feng *et al.* 2014). Thus, autophagy is probably used by *P. involutus* for the recycling of components in the cytoplasm and for maintaining metabolic capacity during C-starvation.

Analysis of the culture medium suggested that peptides were released into the medium by *P. involutus* during C-starvation, particularly during the later stages, and proteolytic activity was detected in the culture medium at the same time. It is known that protease induction in *P. involutus* occurs only in the presence of protein substrate (Shah *et al.* 2013), so our detection of extracellular proteolytic activity is most likely due to the presence of peptides in the medium. Extracellular proteinaceous material is degraded and assimilated in several steps which has been characterized in detail in *P. involutus* (Shah *et al.* 2013). The transcriptome analysis showed that several of those components were significantly upregulated during carbon starvation including extracellular endo- and exopeptidases, as well as several transporters for amino acids and oligopeptides. We found four aspartate endopeptidases to be highly upregulated during the later stages of C-starvation, of which three, the

(a)

Isotig	Prot ID	Description	CS(O)	CS(M)	CS(L)
Hydrolases					
11187	107055	Endopeptidase (A01.019)	0.9	2.1	8.3
3371	169530	Endopeptidase (A01.UPA)	1.3	1.9	2.2
8291	152494	Endopeptidase (A01.UPA)	1.4	1.2	3.2
621	165539	Endopeptidase (A01.UPA)	1.3	1.6	2.4
3479	136623	Carboxypeptidase (S10.UPW)	1.4	2.3	2.7
4176	9113	Carboxylesterase	1.0	0.8	2.8
7949	118603	Carboxylesterase	1.3	1.1	2.3
11739	132242	Carboxylesterase	0.6	0.6	5.0
6318	165902	Lipase (class 3)	1.4	2.1	1.4
6157*	165906	Lipase (class 3)	1.3	2.0	3.5
8947	169306	Nuclease	1.2	1.8	3.5
12266	100682	Glycoside hydrolase (GH10)	2.6	3.5	4.4
6160	70715	Glycoside hydrolase (GH18)	1.9	3.3	2.0
730	66496	Glycoside hydrolase (GH18)	1.7	3.8	4.3
4278	80575	Glycoside hydrolase (GH30)	2.4	2.5	7.3
Oxidases					
9371	76475	Catalase	1.5	2.7	1.7
6210	168806	LPMO (formerly GH61)	2.3	2.5	1.1
2786	100587	Oxidase. FAD linked	1.6	2.1	1.3
11075#	119222	Oxidase. FAD linked	1.4	0.6	6.2
7916	6968	Laccase (AA1_1)	0.9	0.7	2.7
3452§	107098	Laccase (AA1_1)	1.0	1.3	3.1
12273	96078	Laccase (AA1_1)	2.4	3.5	10.0
10764	66942	Laccase (AA1_1)	1.0	1.8	3.0
2772	75212	Oxidase. cytochrome P450	0.8	0.7	2.0
11229	71489	Oxidase. cytochrome P450	1.3	2.5	2.3
Transferases					
5041	173080	Glycosyltransferase (GT22)	1.5	2.0	1.4
6003	63828	Glycosyltransferase (GT59)	1.8	2.5	1.2

(b)

Isotig	Prot ID	Description	CS(O)	CS(M)	CS(L)
7866	168793	Amino acid transporter (APC family)	1.4	1.2	2.6
3844	171086	Amino acid transporter (APC family)	2.0	2.4	2.6
8842	179525	Amino acid transporter (APC family)	1.1	1.3	2.1
7436	167865	Oligopeptide transporter (OPT family)	1.6	1.4	5.2
7617	135671	MSF superfamily (DHA1 family)	0.5	0.8	9.5
4647	78210	MSF superfamily (DHA1 family)	1.1	1.0	7.7
4580/558	94341	MSF superfamily (DHA1 family)	1.2	1.9	3.7
8728	116411	MSF superfamily (DHA1 family)	1.0	1.0	2.1
7808	-	MSF superfamily (DHA2 family)	0.8	1.4	3.6
7650	166126	MSF superfamily (DHA2 family)	1.4	1.3	3.6
550	171941	Ammonium transporter	1.2	1.1	2.0
4631	168886	Anion:cation symporter (ACS family)	1.2	1.8	3.5
4632	168887	Anion:cation symporter (ACS family)	1.2	1.6	2.3
10799	-	Anion:cation symporter (ACS family)	1.1	1.3	2.0

Scale	0.2	1.0	>5.0

Figure 6. Regulation of transcripts predicted to encode extracellular enzymes and nitrogen transporters during C-starvation in *P. involutus*. Shown are the mean fold values ($n = 3$) of such transcripts that were differentially regulated ($q \leq 0.01$, t-test) and upregulated more than 2-fold in at least one of the pair-wise comparisons between mycelium at the onset of C-starvation (CS (O), day 6), after 2 days (CS (M), day 8), and 7 days (CS (L), day 13) of starvation versus actively growing mycelium ((AG), day 2). 'Isotig' refers to transcript ID in the *Paxillus* EST database. 'Prot ID' refers to the predicted protein ID in the *P. involutus* genome. (**a**) Extracellular enzymes. The codes in the parentheses following the peptidase names refer to the ID of the families in the MEROPS peptidase database (Rawlings, Barrett and Bateman 2012), those of glycoside hydrolases and glycoside transferases to the families of the CAZy database (Cantarel *et al.* 2009), and those of auxiliary redox activities/enzymes (Levasseur *et al.* 2013). LPMO indicates lytic polysaccharide monooxygenase. *Expression values shown are the mean of isotigs 6157, 6158 and 11 305 (all these isotigs matched equally well to the sequence of the protein); #the mean of isotigs 11 075, 11 828, 11 741; §the mean of isotigs 3452 and 3450. (**b**) Nitrogen transporters. The transporters are classified according to the system previously described (Saier 2000): APC family, the amino-acid-polyamine-organocation superfamily (TC 2.A.3); OPT family, the oligopeptide transporter superfamily (TC 2.A.67); DHA1, Drug:H^+ antiporter family (TC 2.A.1.2); DHA2, Drug:H^+ antiporter family (TC 2.A.1.3); the ammonium channel transporter family (TC 1.A.11); ACS, the anion:cation symporter family (TC 2.A.1.14).

Gene	Isotig	Prot ID	Description	CS(O)	CS(M)	CS(L)
atg1	7235	132525	Putative autophagy-related serine/threonine kinase (Atg1/ULK complex)	1,5	1,5	1,6
atg13	7375	168678	Regulatory subunit of Atg1 signalling complex (Atg1/ULK complex)	1,2	1,4	1,3
atg17	8815	170997	Scaffold protein of Atg1 signalling complex (Atg1/ULK complex)	1,0	1,4	1,6
atg12	5596*	17541	Ubiquitin-like modifier (Atg12 UB1 conjugation system)	1,1	2,4	6,3
atg16	10601	94501	Atg12-Atg5-Atg16 complex protein (Atg12 UB1 conjugation system)	0,8	0,9	1,3
atg3	4098	137631	E2-like conjugating enzyme (Atg8 UB1 conjugation system)	0,8	0,8	0,8
atg2	6812	162541	Putative membrane protein (Atg9 and its cycling system)	2,5	2,4	2,4
atg9	7193	85915	Transmembrane protein (Atg9 and its cycling system)	1,0	1,2	2,0
atg18	3709#	169336	Phosphoinositide binding protein (Atg9 and its cycling system)	1,1	1,1	1,3
Vps34	7362	171499	Phosphatidylinositol 3-kinase/PI3/PI4-kinase family (PtdIns3K complex)	1,2	1,2	1,6
Vps15	6849	132235	Serine/threonine protein kinase (PtdIns3K complex)	2,0	1,9	1,7
atg24	8512	165381	Sorting nexin (Cvt pathway)	1,1	1,2	1,4
atg27	9799	167257	Type I membrane protein (Cvt pathway)	0,9	1,2	1,7
atg15	874	10303	Vacuolar lipase	0,9	0,8	0,4
atg26	664	123341	UDP-glucose:sterol glucosyltransferase	1,0	1,3	2,0

Scale 0,2 1.0 >5.0

Figure 7. Regulation of transcripts predicted to encode proteins involved in autophagy responses during C-starvation in *P. involutus*. Shown are the mean fold values ($n = 3$) of transcripts that were differentially regulated ($q \leq 0.05$, *t*-test) in at least one of the pair-wise comparisons between mycelium at the onset of C-starvation (CS (O), day 6), after 2 days (CS (M), day 8), and 7 days (CS (L), day 13) of starvation versus actively growing mycelium ((AG), day 2). 'Isotig' refers to transcript ID in the *Paxillus* EST database. 'Prot ID' refers to the predicted protein ID in the *P. involutus* genome.*Expression values shown are the mean of isotigs 5996 and 5995 (the isotigs matched equally well to the sequence of the protein); #the mean of isotigs 3709, 413 and 414.

polyporopepsin (Pi:107055) and the unassigned peptidases Pi:169530 and Pi:165539, were previously found to be significantly upregulated in *P. involutus* during growth on various protein substrates and complex organic matter (Shah *et al.* 2013). Among the starvation-induced N-transporters were a homolog (Pi:168793) of the well-characterized AAT1 transporter of *Amanita muscaria*, which is a high-affinity amino-acid transporter with broad substrate affinity (Nehls *et al.* 1999) as well as a homolog (Pi:171086) to a high-affinity methionine permease in *Laccaria bicolor* (Lucic *et al.* 2008). The coordinated regulations of extracellular peptidases and N-transporters during C-starvation support the hypothesis that proteinaceous material being released from lysed hyphae was recycled by intact parts of the mycelium.

We have recently shown that *P. involutus* has an extensive capacity to degrade complex organic matter using an oxidative mechanism, involving Fenton chemistry similar to that of brown rot wood-decaying fungi (Rineau *et al.* 2012, Rineau *et al.* 2013). Based on homology searches, we identified 267 transcripts in the *P. involutus* EST database that encode enzymes and proteins with a possible role in the degradation of litter material (polysaccharide modifications, aromatic compound degradation, iron reduction, homeostasis and H_2O_2 production) (Rineau *et al.* 2012). In total, 30 of these transcripts were upregulated at least 2-fold during C-starvation in *P. involutus* and 14 of them were also upregulated in *P. involutus* during litter decomposition (Fig. S3, Supporting Information). These transcripts encoded various oxidases [laccases, aromatic peroxygenases, cytochrome P450 oxidases, tyrosinases and AA9 (formerly GH61)], and a benzoquinone reductase. Based on the similarity of the expression profiles between litter decomposition (Rineau *et al.* 2012, 2013) and C-starvation (this study), we hypothesize that a radical-based, oxidative decomposition system is induced during the later stages of the C-starvation in *P. involutus*. Due to the fact that hydroxyl radicals are potent oxidants to a range of different macromolecules including cell wall carbohydrates, membrane lipids, proteins and nucleic acids, the Fenton based decomposing pathway may be of key importance for the recycling of the cellular material that is released during the autolysis of the C-starved mycelium of *P. involutus*.

The EMM comprise a considerable part of the microbial biomass in forest soils (Högberg and Högberg 2002), and recent studies suggest that the mycelium has a major impact on C-cycling by influencing decomposition as well as formation of soil organic matter (Lindahl and Tunlid 2015). Likely autolysis following C-starvation represents an important pathway leading to the release of mycelial derived material into the soil organic matter pool. The molecular signatures identified in this study can be used as markers to examine this hypothesis in more complex soil systems, and ultimately in the field.

SUPPLEMENTARY DATA

Supplementary data is available at FEMSEC online.

ACKNOWLEDGEMENTS

We thank Dr. Francis Martin for support with the genome sequencing project of *P. involutus*.

FUNDING

The work was supported by grants from the Swedish Research Council (VR) and the strategic research program Biodiversity and Ecosystem Services in a Changing Climate (BECC). Genome sequencing was conducted by the US Department of Energy Joint Genome Institute, supported by the Office of Science of the US Department of Energy under Contract No. DE-AC02-05CH1123.1.

Conflict of interest. None declared.

REFERENCES

Apweiler R, Bairoch A, Wu CH, *et al.* UniProt: the Universal Protein knowledgebase. *Nucleic Acids Res* 2004;**32**:D115–9.

Arnebrant K. Nitrogen amendments reduce the growth of extramatrical ectomycorrhizal mycelium. *Mycorrhiza* 1994;**5**:7–15.

Arnebrant K, Söderström B. Effects of different fertilizer treatments on ectomycorrhizal colonization potential in 2 Scots pine forests in Sweden. *Forest Ecol Manag* 1992;**53**:77–89.

Bahr A, Ellström M, Akselsson C, *et al.* Growth of ectomycorrhizal fungal mycelium along a Norway spruce forest nitrogen deposition gradient and its effect on nitrogen leakage. *Soil Biol Biochem* 2013;**59**:38–48.

Ball CA, Brazma A, Causton H, *et al.* Submission of microarray data to public repositories. *PLoS Biol* 2004;**2**:1276–7.

Barth A. Infrared spectroscopy of proteins. *BBA-Bioenergetics* 2007;**1767**:1073–101.

Benjamini Y, Hochberg Y. Controlling the false discovery rate: a practical and powerful approach to multiple testing. *J Roy Stat Soc B*1995;**57**:289–300.

Bolstad BM, Irizarry RA, Åstrand M, *et al.* A comparison of normalization methods for high density oligonucleotide array data based on variance and bias. *Bioinformatics* 2003;**19**:185–93.

Brugnerotto J, Lizardi J, Goycoolea FM, *et al.* An infrared investigation in relation with chitin and chitosan characterization. *Polymer* 2001;**42**:3569–80.

Cantarel BL, Coutinho PM, Rancurel C, *et al.* The Carbohydrate-Active EnZymes database (CAZy): an expert resource for Glycogenomics. *Nucleic Acids Res* 2009;**37**:D233–8.

Chalot M, Blaudez D, Brun A. Ammonia: a candidate for nitrogen transfer at the mycorrhizal interface. *Trends Plant Sci* 2006;**11**:263–6.

Colthup NB, Daly LH, Wiberley SE. *Introduction to Infrared and Raman Spectroscopy*. San Diego, CA: Academic Press, 1990.

Dietz S, von Buelow J, Beitz E, *et al.* The aquaporin gene family of the ectomycorrhizal fungus *Laccaria bicolor*: lessons for symbiotic functions. *New Phytol* 2011;**190**:927–40.

Eastwood DC, Floudas D, Binder M, *et al.* The plant cell wall-decomposing machinery underlies the functional diversity of forest fungi. *Science* 2011;**333**:762–5.

Edgar R, Domrachev M, Lash AE. Gene Expression Omnibus: NCBI gene expression and hybridization array data repository. *Nucleic Acids Res* 2002;**30**:207–10.

Ekblad A, Wallander H, Godbold DL, *et al.* The production and turnover of extramatrical mycelium of ectomycorrhizal fungi in forest soils: role in carbon cycling. *Plant Soil* 2013;**366**:1–27.

Ericsson T. Growth and shoot: root ratio of seedlings in relation to nutrient availability. *Plant Soil* 1995;**168–9**:205–14.

Feng Y, He D, Yao Z, *et al.* The machinery of macroautophagy. *Cell Res* 2014;**24**:24–41.

Finn RD, Bateman A, Clements J, *et al.* Pfam: the protein families database. *Nucleic Acids Res* 2014;**42**:D222–30.

Guaragnella N, Butow RA. ATO3 encoding a putative outward ammonium transporter is an RTG-independent retrograde responsive gene regulated by GCN4 and the Ssy1-Ptr3-Ssy5 amino acid sensor system. *J Biol Chem* 2003;**278**:45882–7.

Högberg MN, Briones MJI, Keel SG, *et al.* Quantification of effects of season and nitrogen supply on tree below-ground carbon transfer to ectomycorrhizal fungi and other soil organisms in a boreal pine forest. *New Phytol* 2010;**187**:485–93.

Högberg MN, Högberg P. Extramatrical ectomycorrhizal mycelium contributes one-third of microbial biomass and produces, together with associated roots, half the dissolved organic carbon in a forest soil. *New Phytol* 2002;**154**:791–5.

Irizarry RA, Bolstad BM, Collin F, *et al.* Summaries of affymetrix GeneChip probe level data. *Nucleic Acids Res* 2003;**31**:e15.

Kohler A, Kuo A, Nagy LG, *et al.* Convergent losses of decay mechanisms and rapid turnover of symbiosis genes in mycorrhizal mutualists. *Nat Genet* 2015, DOI: 10.1038/ng.3223.

Kjøller R, Nilsson LO, Hansen K, *et al.* Dramatic changes in ectomycorrhizal community composition, root tip abundance and mycelial production along a stand-scale nitrogen deposition gradient. *New Phytol* 2012;**194**:278–86.

Leake JR, Donnelly DP, Saunders EM, *et al.* Rates and quantities of carbon flux to ectomycorrhizal mycelium following C-14 pulse labeling of *Pinus sylvestris* seedlings: effects of litter patches and interaction with a wood-decomposer fungus. *Tree Physiol* 2001;**21**:71–82.

Levasseur A, Drula E, Lombard V, *et al.* Expansion of the enzymatic repertoire of the CAZy database to integrate auxiliary redox enzymes. *Biotechnol Biofuels* 2013;**6**:1–14.

Lindahl BD, Tunlid A. Ectomycorrhizal fungi—potential organic matter decomposers, yet not saprophytes. *New Phytol*, 2015;**205**:1443–7.

Lucic E, Fourrey C, Kohler A, *et al.* A gene repertoire for nitrogen transporters in *Laccaria bicolor*. *New Phytol* 2008;**180**:343–64.

Nehls U, Kleber R, Wiese J, *et al.* Isolation and characterization of a general amino acid permease from the ectomycorrhizal fungus *Amanita muscaria*. *New Phytol* 1999;**144**:343–9.

Nitsche B, Jørgensen T, Akeroyd M, *et al.* The carbon starvation response of *Aspergillus niger* during submerged cultivation: Insights from the transcriptome and secretome. *BMC Genomics* 2012;**13**:380.

Nitsche BM, Burggraaf-van Welzen A-M, Lamers G, *et al.* Autophagy promotes survival in aging submerged cultures of the filamentous fungus *Aspergillus niger*. *Appl Microbiol Biot* 2013;**97**:8205–18.

Petersen TN, Brunak S, von Heijne G, *et al.* SignalP 4.0: discriminating signal peptides from transmembrane regions. *Nat Methods* 2011;**8**:785–6.

Plassard CS, Mousain DG, Salsac LE. Estimation of mycelial growth of basidiomycetes by means of chitin determination. *Phytochemistry* 1982;**21**:345–8.

Pocsi I, Pusztahelyi T, Sami L, *et al.* Autolysis of *Penicillium chrysogenum*: A holistic approach. *Indian J Biotechnol* 2003;**2**:293–301.

Pollack JK, Harris SD, Marten MR. Autophagy in filamentous fungi. *Fungal Genet Biol* 2009;**46**:1–8.

Rawlings ND, Barrett AJ, Bateman A. MEROPS: the database of proteolytic enzymes, their substrates and inhibitors. *Nucleic Acids Res* 2012;**40**:D343–50.

Rineau F, Roth D, Shah F, *et al.* The ectomycorrhizal fungus *Paxillus involutus* converts organic matter in plant litter using a trimmed brown-rot mechanism involving Fenton chemistry. *Environ Microbiol* 2012;**14**:1477–87.

Rineau F, Shah F, Smits MM, *et al.* Carbon availability triggers the decomposition of plant litter and assimilation of nitrogen by an ectomycorrhizal fungus. *ISME J* 2013;**7**:2010–22.

Saier MH. A functional-phylogenetic classification system for transmembrane solute transporters. *Microbiol Mol Biol R* 2000;**64**:354–411.

Sami L, Karaffa L, Emri T, *et al.* Autolysis and ageing of *Penicillium chrysogenum* under carbon starvation: Respiration and glucose oxidase production. *Acta Microbiol Imm H* 2003;**50**:67–76.

Schrickx JM, Krave AS, Verdoes JC, *et al.* Growth and product formation in chemostat and recycling cultures by *Aspergillus niger* N402 and a glucoamylase overproducing transformant,

provided with multiple copies of the glaA gene. *J Gen Microbiol* 1993;**139**:2801–10.

Shah F, Rineau F, Canbäck B, *et al*. The molecular components of the extracellular protein-degradation pathways of the ectomycorrhizal fungus *Paxillus involutus*. *New Phytol* 2013;**200**:875–87.

Sharon A, Finkelstein A, Shlezinger N, *et al*. Fungal apoptosis: function, genes and gene function. *FEMS Microbiol Rev* 2009;**33**:833–54.

Shin K-S, Kwon N-J, Kim YH, *et al*. Differential roles of the ChiB chitinase in autolysis and cell death of *Aspergillus nidulans*. *Eukaryot Cell* 2009;**8**:738–46.

Smith SE, Read DJ. *Mycorrhizal Symbiosis*. London: Academic Press, 2008.

Szilagyi M, Miskei M, Karanyi Z, *et al*. Transcriptome changes initiated by carbon starvation in *Aspergillus nidulans*. *Microbiology* 2013;**159**:176–90.

Trinci APJ, Righelato RC. Changes in constituents and ultrastructure of hyphal compartments during autolysis of glucose starved *Penicillium chrysogenum*. *J Gen Microbiol* 1970;**60**:239–49.

Tsuji A, Kinoshita T, Hoshino M. Analytical chemical studies on amino sugars. II. Deterimation of hexosamines using 3-Methyl-2-benzothiazolone Hydrazone Hydrochloride. *Chem Pharm Bull* 1969;**17**:1505–10.

Twining SS. Fluorescein isothiocyanate-labeled casein assay for proteolytic-enzymes. *Anal Biochem* 1984;**143**:30–4.

Wallander H, Nylund JE. Effects of excess nitrogen and phosphorus starvation on the extramatrical mycelium of ectomycorrhizas of *Pinus sylvestris* L. *New Phytol* 1992;**120**:495–503.

Wallander H, Söderström B. Paxillus. In: Cairney JWG, Chambers SM (eds). *Ectomycorrhizal Fungi: Key Genera in Profile*. Berlin, UK: Springer, 1999, 231–52.

White S, McIntyre M, Berry DR, *et al*. The autolysis of industrial filamentous fungi. *Crit Rev Biotechnol* 2002;**22**:1–14.

Voigt O, Poeggeler S. Self-eating to grow and kill: autophagy in filamentous ascomycetes. *Appl Microbiol Biot* 2013;**97**:9277–90.

Yamashita Y, Tanoue E. Chemical characterization of protein-like fluorophores in DOM in relation to aromatic amino acids. *Mar Chem* 2003;**82**:255–71.